Semaphorin3A Enhances Endocytosis at Sites of Receptor–F-actin Colocalization during Growth Cone Collapse

Alyson E. Fournier,[*][‡] **Fumio Nakamura,**[*][‡] **Susumu Kawamoto,**[||] **Yoshio Goshima,**[¶] **Robert G. Kalb,**[*][§] **and Stephen M. Strittmatter**[*][‡]

[*]Department of Neurology, [‡]Department of Neurobiology, [§]Department of Pharmacology, Yale University School of Medicine, New Haven, Connecticut 06520; and [||]Department of Bacteriology, [¶]Department of Pharmacology, Yokohama City University School of Medicine, Yokohama 236, Japan

Abstract. Axonal growth cone collapse is accompanied by a reduction in filopodial F-actin. We demonstrate here that semaphorin 3A (Sema3A) induces a coordinated rearrangement of Sema3A receptors and F-actin during growth cone collapse. Differential interference contrast microscopy reveals that some sites of Sema3A-induced F-actin reorganization correlate with discrete vacuoles, structures involved in endocytosis. Endocytosis of FITC-dextran by the growth cone is enhanced during Sema3A treatment, and sites of dextran accumulation colocalize with actin-rich vacuoles and ridges of membrane. Furthermore, the Sema3A receptor proteins, neuropilin-1 and plexin, and the Sema3A signaling molecule, rac1, also reorganize to vacuoles and membrane ridges after Sema3A treatment. These data support a model whereby Sema3A stimulates endocytosis by focal and coordinated rearrangement of receptor and cytoskeletal elements. Dextran accumulation is also increased in retinal ganglion cell (RGC) growth cones, in response to ephrin A5, and in RGC and DRG growth cones, in response to myelin and phorbol-ester. Therefore, enhanced endocytosis may be a general principle of physiologic growth cone collapse. We suggest that growth cone collapse is mediated by both actin filament rearrangements and alterations in membrane dynamics.

Key words: membrane dynamics • ephrins • dextran uptake • axon guidance • axon repulsion

Introduction

Axonal pathfinding during neuronal development is mediated by the growth cone, which integrates and responds to guidance cues in the environment. Growth cones are thought to respond to extracellular cues by selectively stabilizing or destabilizing the actin cytoskeleton in filopodia and lamellipodia to achieve directional growth (Bentley and O'Connor, 1994; Lin et al., 1994). Both attractive and repulsive environmental cues, including the semaphorin family of growth cone collapsing factors (Puschel, 1996) affect growth cone morphology (Goodman, 1996). Repulsive agents can either completely collapse growth cones and arrest neurite outgrowth or cause asymmetric growth cone collapse and growth cone steering (Fan and Raper, 1995; Song et al., 1998).

Many studies examining the mechanism of axon repulsion have focused on the collapse response to Sema3A (SemD, collapsin-1, and semaIII), a member of the class 3 semaphorin family that repulses the axons of sensory and sympathetic neurons (Luo et al., 1993). Semaphorin 3A (Sema3A)[1]–induced growth cone collapse has been described as a process whereby lamellar protrusion and filopodial motility are paralyzed before the retraction of all growth cone specializations (Fan et al., 1993). Collapse is accompanied by a 50% net loss of F-actin from the leading edge of the growth cone. The morphological response to Sema3A is similar to that caused by cytochalasin B, a plant alkaloid that inhibits actin polymerization, paralyzes normal growth cone motility, and inhibits axonal extension (Letourneau et al., 1987). Raper and colleagues concluded that the collapse of the growth cone structure is attributable to this reduction in F-actin concentration (Fan et al., 1993).

Address correspondence to Stephen M. Strittmatter, Department of Neurology, Yale University School of Medicine, 333 Cedar Street, P.O. Box 208018, New Haven, CT 06520. Tel.: (203) 785-4878. Fax: (203) 785-5098. E-mail: stephen.strittmatter@yale.edu

[1]*Abbreviations used in this paper:* DIC, differential interference contrast; DRG, dorsal root ganglia; NP, neuropilin; RGC, retinal ganglion cell; Sema3A, semaphorin 3A; Sema3C, semaphorin 3C; TPA, phorbol-12 myristate 13-acetate.

Since these initial studies, several molecules in the Sema3A signaling pathway have been identified. The axonal glycoprotein neuropilin-1 (NP-1) has been identified as the high affinity binding site for Sema3A (He and Tessier-Lavigne, 1997; Kolodkin et al., 1997). The transmembrane protein plexin A1 associates with NP-1 and is responsible for the intracellular transduction of a Sema3A signal (Takahashi et al., 1999; Tamagnone et al., 1999). Further, collapsin response mediator proteins (CRMPs) and rac1 have been implicated in the Sema3A signaling pathway. Treatment of neurons with either anti–CRMP-62 antibodies (Goshima et al., 1995) or dominant negative rac1 (Jin and Strittmatter, 1997; Kuhn et al., 1999) prevents growth cone collapse by Sema3A.

To further our understanding of the mechanism of growth cone collapse, we examined the distribution of F-actin, NP-1, plexin, and rac1 in dorsal root ganglia (DRG) growth cones at different stages of collapse after treatment with Sema3A. We observe that F-actin, NP-1, plexin, and rac1 are redistributed in a coordinated fashion to new membrane ridges and vacuoles after Sema3A treatment. Because F-actin–based formation of similar structures is a key element for some endocytic pathways, we examined the effect of Sema3A on fluid phase endocytosis. We demonstrate that Sema3A stimulates endocytosis, and that this event correlates with growth cone collapse. Furthermore, multiple inhibitors of axon extension stimulate fluid phase endocytosis in both DRG and retinal ganglion cell (RGC) growth cones. These observations suggest that both coordinated cytoskeletal reorganization and endocytosis contribute to growth cone collapse.

Materials and Methods

Preparation of Proteins

Sema3A (collapsin-His$_6$) and Sema3C were prepared as previously described (Goshima et al., 1995; Takahashi et al., 1998). Cytochalasin B and phorbol-12 myristate-13 acetate (TPA; Sigma Chemical Co.) were used at concentrations of 2 and 1 μM, respectively. Purified recombinant L1Fc (Doherty et al., 1995) was used at a concentration of 5 μg/ml. L1Fc activity was verified by treating dissociated DRG neurons with 5 μg/ml L1Fc for 20 h. This treatment enhanced DRG neurite outgrowth on laminin by 75%. Myelin extracts were prepared from the bovine brain as previously described (Igarashi et al., 1993). After clarification of the myelin extract by centrifugation at 400,000 g, the detergent was removed by dialysis against Ham's F12 medium. Myelin was used at a concentration of 50 μg protein/ml. Membrane preparations containing RAGS were prepared as described for tectal membrane fragments (Walter et al., 1987; Drescher et al., 1995). High five insect cells were pelleted 2 d after infection with an ephrin A5–expressing baculovirus. The cell pellet was resuspended in homogenization buffer with protease inhibitors (10 mM Tris-HCl, pH 7.4, 1.5 mM CaCl$_2$, 1 mM PMSF, 200 k.u./ml aprotinin, 20 μM leupeptin) and lysed by sonication. Nuclei and cytoplasm were removed by centrifugation. The homogenate was layered on top of a sucrose cushion of 50 and 5% sucrose solutions and centrifuged for 10 min at 20,000 g. Plasma membrane fragments were collected from the turbid layer formed at the boundary between the 5 and 50% sucrose solutions. Preparations were stored in 60-μg aliquots at -80°C. For use in growth cone collapse assays, membrane preparations were pelleted, resuspended in F12, sonicated, and applied to cultures at 30 μg protein/ml to induce growth cone collapse. Such preparations collapsed >80% of chick E7 RGC growth cones.

Neuronal Culture and Immunohistology

Chick E7 DRG and retinal explants were cultured in growth medium (F12 medium with 10% FBS, 50 ng/ml 7S-NGF, 10 U/ml penicillin and streptomycin) for 18 h on 4-well glass chamber slides precoated sequentially with 100 μg/ml poly-L-lysine and with 10 μg/ml laminin. After experimental manipulations, explants were fixed by adding ice-cold 4% paraformaldehyde, 20% sucrose, and 0.1 M NaPO$_4$, pH 7.3, directly to the medium.

For immunocytochemical staining, explants were stained with either Rac1 mAb (UBI; 4 μg/ml), NP-1 polyclonal antibody (a gift from H. Fujisawa, Nagoya University Graduate School of Science, Nagoya, Japan), plexin polyclonal antibody (Takahashi et al., 1999), or GAP-43 polyclonal antibody (Sigma Chemical Co.), followed by a fluorescein- or rhodamine-conjugated secondary antibody (1 μg/ml). To visualize actin filaments, explants were stained with rhodamine-phalloidin (0.33 μM; Molecular Probes).

FITC-Dextran Uptake

For FITC-dextran uptake assays, half of the DRG medium (250 μl) was replaced with prewarmed fresh medium containing 2 mg FITC-dextran per milliliter (Molecular Probes) and the collapsing agent to be tested. Explants were incubated at 37°C for 5–120 min, gently washed with prewarmed DRG medium without dextran, and were fixed. To stain the total protein, explants were permeabilized in 0.5% Triton X-100, and a 1% solution of TRITC (Sigma Chemical Co.) in DMSO was diluted 1,000-fold into PBS immediately before use (Fan et al., 1993). Preparations were stained with TRITC for 15 min, rinsed in PBS, and mounted in gelmount (Fisher Scientific Co.).

Growth cones were viewed on a fluorescence microscope with a 60× objective (1.4 NA) and an AstroCam camera. For quantification, matched fluorescein (dextran) and rhodamine (total protein) digital images were analyzed using the Scion version of NIH Imager. The growth cone (defined as the distal 75 μm of the axon) was outlined according to the rhodamine image (total protein), and the mean fluorescence intensity per pixel was measured in each fluorescence channel. Dextran levels were calculated as follows:

$$\frac{\text{FITC mean intensity per pixel} - \text{FITC background}}{\text{TRITC mean intensity per pixel} - \text{TRITC background}}.$$

Dextran levels in the presence of test compounds were normalized against the value for control growth cones of the same time point in the same experiment. Dextran levels without test compounds were low and varied only slightly between 5–120 min. Error bars reflect the SEM from 3 to 10 independent experiments.

Results

Sema3A Stimulates the Formation of Discrete F-actin–positive Structures

To gain insight into Sema3A signaling mechanisms, we examined the spatial organization of F-actin during Sema3A-induced growth cone collapse. E7 chick DRG explants were treated with Sema3A, fixed at different stages of growth cone collapse, and were stained with rhodamine-phalloidin to detect F-actin. Cultures were viewed by DIC and fluorescence microscopy to visualize growth cone morphology and F-actin staining (Fig. 1). Control growth cones are well spread, and F-actin staining is diffuse in lamellipodia and intense in filopodia (Fig 1, a and b). After Sema3A treatment, F-actin staining rapidly redistributes into punctate aggregates throughout the lamellipodia of the growth cone (Fig. 1, c and e). Redistribution of F-actin into aggregates is visible as early as 2 min after Sema3A treatment, a time when most growth cones remain well spread. Further, F-actin is rapidly lost from growth cone filopodia in response to Sema3A. DIC imaging illustrates that collapsing growth cones often retain filopodial structures that are devoid of F-actin. By 5 min after Sema3A treatment, F-actin labels discrete circular profiles (Fig. 1 g). Some circular profiles are similar to the reverse shadowcast vacuoles previously reported by Dailey and Bridgman (1993) in a correlative electron microscopy
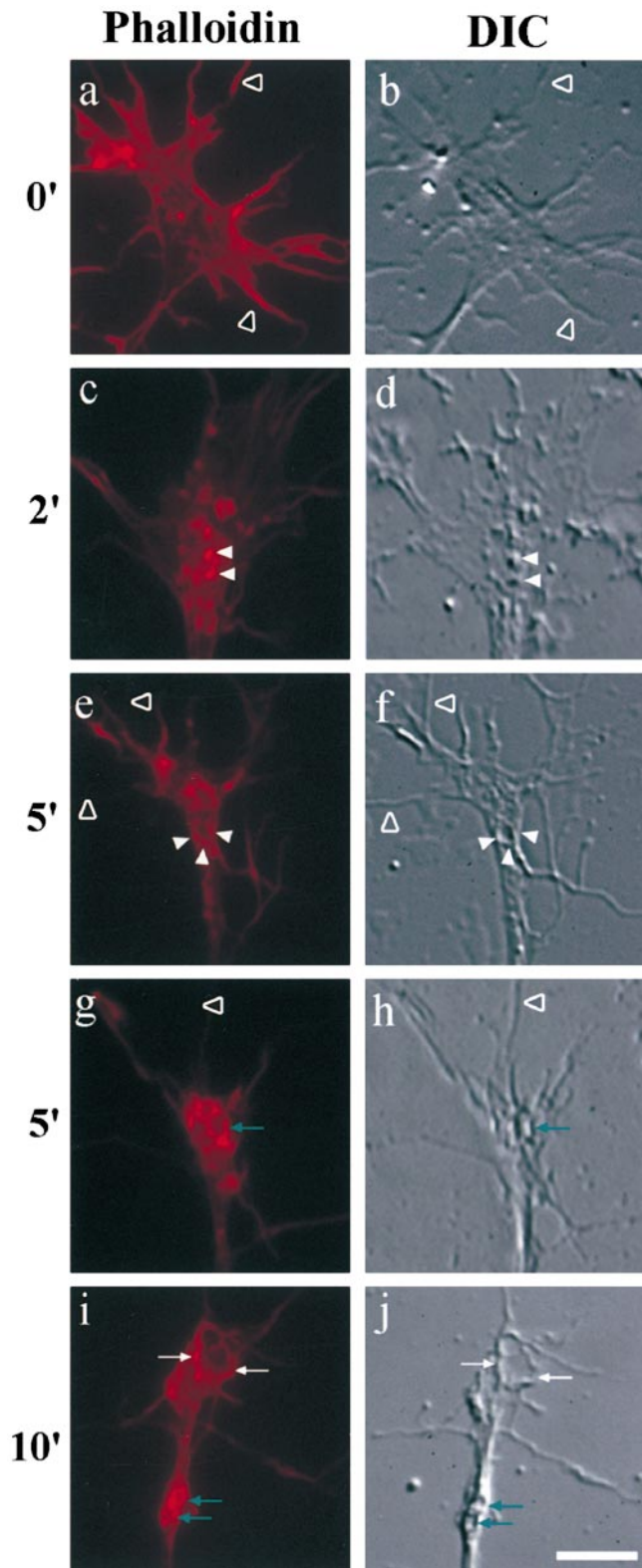
Phalloidin DIC

0' a ◁ | b ◁

◁ | ◁

2' c | d
▼▼ | ▼▼

5' e ◁ | f ◁
△ | △
▼▼▼ | ▼▼▼

5' g ◁ | h ◁
→ | →

10' i | j
→ → | → →
→ | →
→ |

Figure 1. Sema3A induces F-actin redistribution in growth cones. Chick E7 DRG cultures were treated for 0–10 min with 1 nM of Sema3A and visualized by DIC and fluorescence microscopy. Growth cones were stained with phalloidin to detect F-actin. Matched images of growth cones visualized by DIC and F-actin labeling demonstrate that F-actin is concentrated in the filopodia (open arrowheads) of control growth cones, and diffusely stains the central domain and lamellipodia (a and b). After Sema3A

and DIC study of untreated neuronal growth cones (Fig. 1 f; see also Fig. 7, b, e, and k). However, often the circular profiles are delineated by edges that protrude from the plane of the growth cone membrane (Fig. 1 h; see also 7, b and e). Occasionally, punctate aggregates of F-actin seem to outline circular profiles within the growth cone (Fig. 1, e and f). In addition to vacuolar structures, F-actin–positive linear ridges are visible in Sema3A-treated growth cones (Fig. 1, i and j). Time lapse observations of unfixed growth cones by DIC microscopy (data not shown) reveals that the linear profiles of material are highly motile membrane ridges that form in the lamellipodia of the growth cone after Sema3A treatment. The membrane ridges rapidly (60 s) flow across the lamellipodium surface in a fashion consistent with the membrane ruffling discovered in other cells. Our observations of F-actin in Sema3A-treated growth cones confirm the loss of the peripheral F-actin reported by Fan et al. (1993), but also demonstrate a coordinated rearrangement of F-actin into discrete structures within the growth cone lamellipodium in response to Sema3A.

To examine if the formation of these new growth cone structures are driven by Sema3A signaling, we examined the distribution of NP-1 and plexin, which are members of the Sema3A receptor complex, and of rac1, which is a member of the Sema3A signaling pathway (Fig. 2). In response to Sema3A treatment, NP-1, plexin, and rac1 codistribute with newly formed F-actin–rich structures. Each of these signaling molecules demonstrates reorganization to aggregates, ridges, and vacuoles. The examples in Fig. 2 demonstrate rac redistribution to punctate aggregates, NP-1 redistribution around a circular profile, and plexin redistribution to a linear ridge. Sema3A-treated growth cones were also double stained with phalloidin and GAP-43. GAP-43 is a phosphoprotein that is localized to the inner membrane of the neuronal growth cone via palmitoylation, but is not thought to be involved in Sema3A action (Liu et al., 1993). GAP-43 does not associate with F-actin–rich structures after Sema3A treatment (Fig. 2). The absence of GAP-43 staining in the presence of Sema3A-induced F-actin rearrangements demonstrates that the reorganization of NP-1, plexin, and rac1 are not artifacts because of the effects of increased cytoplasmic volume at these sites.

Sema3A Stimulates Fluid Phase Endocytosis

The recruitment of F-actin to the surface of membrane specializations has been correlated with fluid phase pinocytosis in nonneuronal cells (Bar-sagi and Feramisco, 1986), and actin accumulations are correlated with type I phagocytosis (Caron and Hall, 1998). This prompted us to consider the effect of Sema3A on endocytosis during DRG growth cone collapse (Fig. 3). Growth cones were exposed to Sema3A in the presence of FITC-conjugated dextran. Control growth cones exposed to FITC-dextran show light dextran labeling reflecting low basal levels of endocytosis (Fig. 3 e). After Sema3A treatment, a large accumulation of FITC-dextran is evident in the growth cone tip within 5 min (Fig. 3 h). By 20 min after Sema3A

treatment, F-actin rapidly reorganizes into punctate aggregates (white arrowheads), linear membrane ridges (white arrows), and large vacuoles (green arrows). Bar, 15 μm.
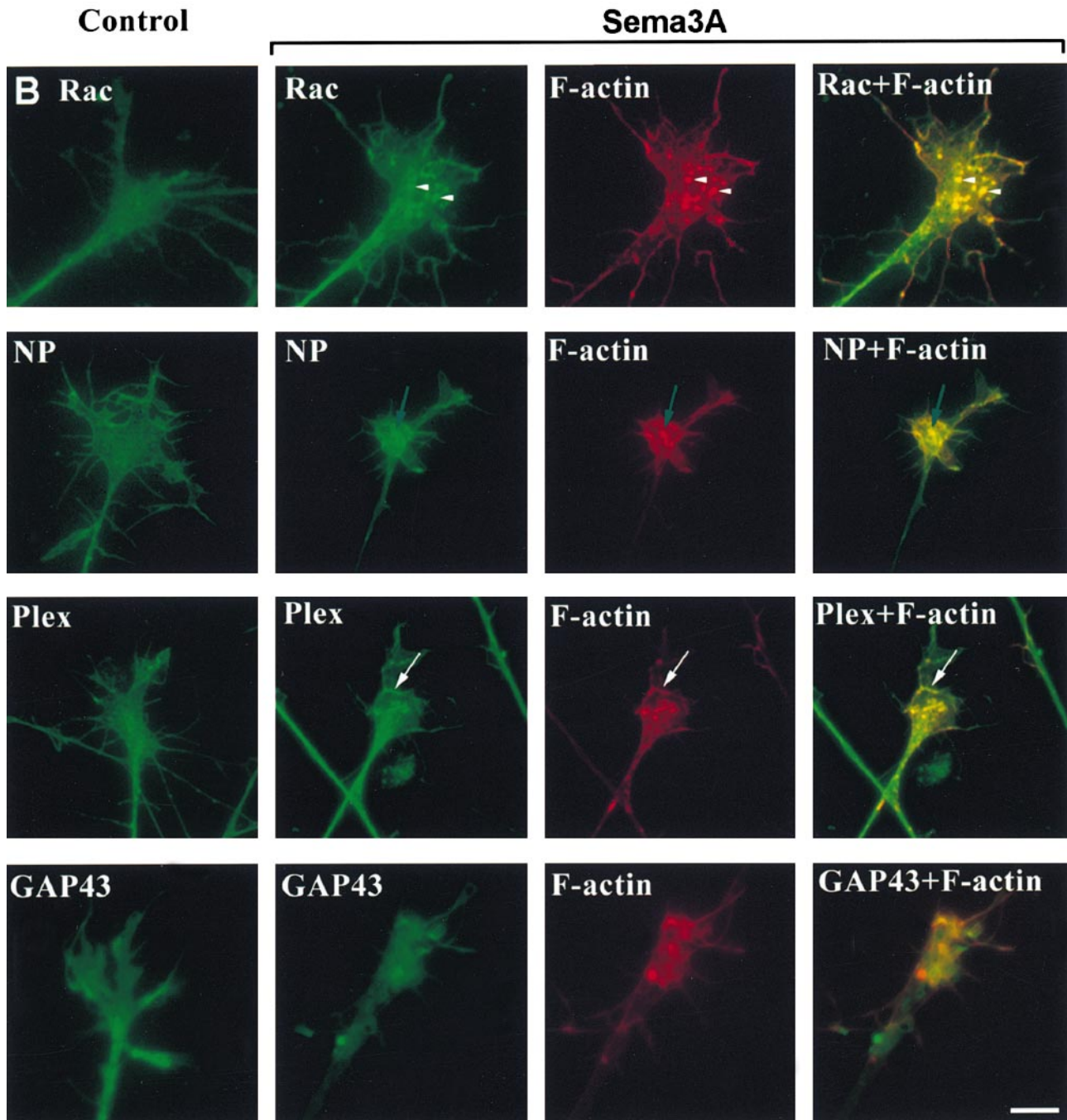
Figure 2. Sema3A induces Rac1, NP1, and plexin redistribution in growth cones. Chick E7 cultures were treated for 0–10 min with 1 nM Sema3A, and were visualized by fluorescence microscopy. Growth cones were double stained with phalloidin to detect F-actin and antibodies against Rac1, neuropilin-1 (NP), plexin (Plex), or GAP-43. NP-1, plexin, and Rac1 reorganize to sites of F-actin reorganization during collapse. GAP-43 does not redistribute to F-actin–positive structures after Sema3A treatment. Bar, 20 μm.

application, dextran accumulations are detectable in a more proximal portion of the axon (Fig. 3 k), presumably because of retrograde transport. By 2 h, dextran labeling is no longer visible (Fig. 3 n). The observed endocytic dextran accumulation reflects the sum of dextran uptake, secretion, and removal from the growth cone by retrograde transport. However, previous studies have indicated that Sema3A increases retrograde vesicular axonal transport

(Goshima et al., 1997), which would only decrease dextran accumulation in the growth cone. Thus, decreased removal is an improbable explanation for Sema3A-induced growth cone dextran accumulation. Dextran accumulation during brief incubation periods is likely to reflect primarily changes in uptake rates since initially there is no labeled endocytic pool from which secretion or removal might be altered. Furthermore, accumulation is not greater at later
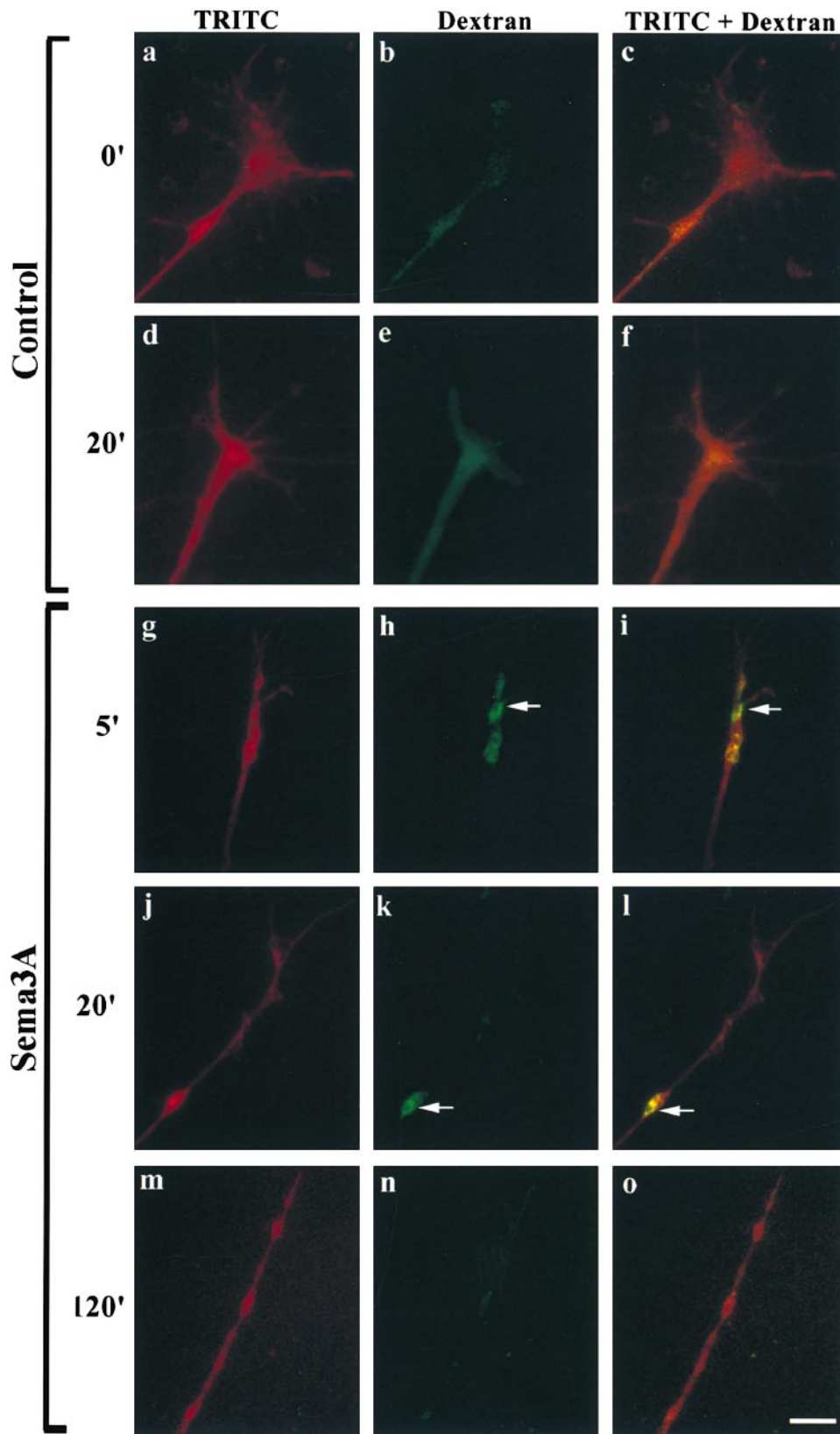
Figure 3. Sema3A stimulates fluid phase endocytosis. E7 chick DRG growth cones were incubated with medium (a–f) or Sema3A (g–o) in the presence of FITC-dextran. Dextran is visualized through the FITC channel (b, e, h, k, and n). Growth cones were counterstained with TRITC to label the total protein in the growth cone (a, d, g, j, and m). Merged images (c, f, i, l, and o) demonstrate dextran concentrations (arrows) relative to the total protein. In a control growth cone, treated with dextran only, labeling is weak and diffuse (e), however, dextran accumulates 5 min after Sema3A treatment and brightly labels the collapsing growth cone (h). After 20 min in the presence of Sema3A, dextran is often retrogradely transported into the neurite shaft (k) and, by 2 h, dextran is no longer present within the growth cone or neurite (n). Bar, 20 μm.

time points when any secretion effects should be more prominent.

To consider whether endocytosis is stimulated by nonligand-mediated growth cone collapse, we examined FITC-dextran accumulation during cytochalasin B treatment. Cytochalasin B is a plant alkaloid that stimulates growth cone collapse, which is morphologically similar to that elicited by Sema3A. Cytochalasin B inhibits actin po-

lymerization, paralyzes normal growth cone motility, and inhibits axonal extension (Letourneau et al., 1987). We find that treatment of DRG growth cones with cytochalasin B induces rapid growth cone collapse, but does not enhance dextran accumulation (Fig. 4, a–c; see also Fig. 5 c). This suggests that stimulated dextran accumulation is not simply a consequence of changing morphology during growth cone collapse or a secondary effect of actin loss from growth cone filopodia. Rather, it appears that endocytosis is actively stimulated by Sema3A.

In addition to growth cone collapsing agents, we examined the effect of a growth promoting ligand on dextran accumulation by treating DRGs with L1 glycoprotein. L1 is a cell adhesion molecule expressed by a variety of mammalian neurons, and homophilic L1 interactions on adjacent cells can promote axonal outgrowth (Seilheimer and Schachner, 1988). To test the effect of L1 on dextran accumulation, we treated DRG neurons with a soluble L1Fc chimeric molecule that also stimulates neurite outgrowth (Doherty et al., 1995). Treatment of dissociated DRGs with L1Fc protein at 5 μg/ml enhances neurite outgrowth by 50–75% (Archer et al., 1999; data not shown). DRG growth cones treated with L1Fc for 5 min (Fig. 4, d–f; see also Fig. 5 c) or 20 min (data not shown) remain well spread and do not exhibit enhanced levels of dextran accumulation.

We quantified the dextran levels relative to the total protein in the collapsing growth cone to ensure that brighter dextran levels are not due to changes in the thickness of the collapsing growth cone. Similar to the methodology employed by Fan et al. (1993), total protein within the growth cone was labeled with TRITC, and the total dextran per unit area was measured relative to the total protein per unit area in the growth cone (Fig. 5). We find that the dextran levels throughout the growth cone are elevated to ~300% of control levels by 5 min after Sema3A treatment, and return to the baseline by 2 h after Sema3A treatment. Focal accumulations are much higher than this average value. For several different incubation times and doses, dextran accumulation correlates with growth cone collapse (Fig. 5, a and b). Both Sema3C, which binds to NP-1 but does not repel DRG neurons (Takahashi et al., 1998), and ephrin A5, which causes collapse of RGCs but not DRG growth cones (Drescher et al., 1995), fail to stimulate dextran accumulation in DRGs (Fig. 5 c).

Ligand-stimulated Endocytosis Correlates with Growth Cone Collapse

To examine the extent to which endocytosis is a general principle of physiologic growth cone collapse, we assessed the ability of other growth cone collapsing agents to stimulate fluid phase endocytosis. We tested central nervous system myelin extracts, which contain multiple outgrowth inhibitors including MAG (McKerracher et al., 1994) and Nogo (Caroni and Schwab, 1988; Chen et al., 2000; Grandpre et al., 2000; Prinjha et al., 2000), which stimulate growth cone collapse (Bandtlow et al., 1993; Li et al., 1996). In addition, we tested TPA, an activator of protein kinase C, which potently stimulates DRG growth cone collapse at concentrations as low as 10 nM (data not shown). For DRG growth cones, both myelin and TPA stimulate FITC-dextran accumulation (Fig. 5 d). Similar to Sema3A, dextran accumulation is strongly stimulated in the growth cone tip within 5 min of ligand treatment, and is diminished 20 min after stimulation when the dextran is found in a more distal portion of the axon.
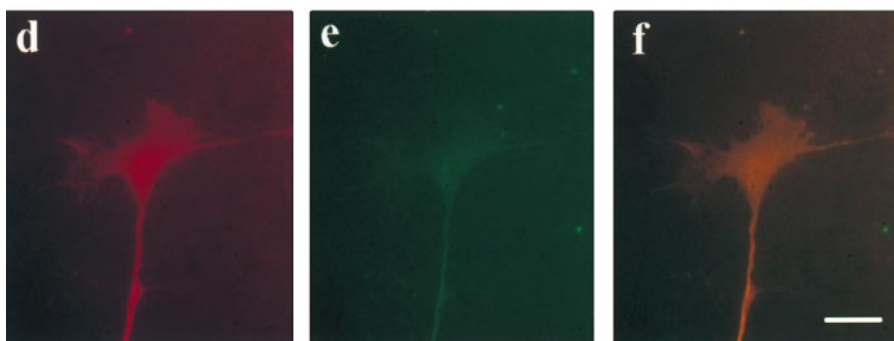
Cytochalasin
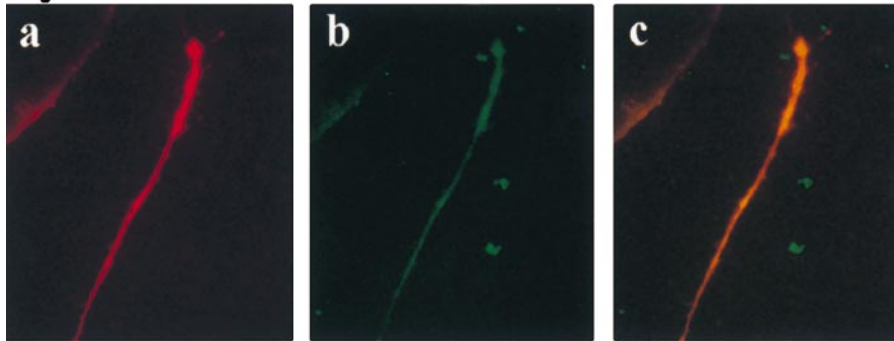
L1

Figure 4. Cytochalasin and L1 fail to stimulate fluid phase endocytosis. E7 chick DRG growth cones were incubated with 2 μM cytochalasin B (a–c) or 5 μg/ml L1 (d–f) for 5 min in the presence of FITC-dextran. Dextran is visualized through the FITC channel (b and e). Growth cones were counterstained with TRITC to label the total protein in the growth cone (a and d). Merged images (c and f) demonstrate dextran staining relative to total protein. Cytochalasin B stimulates growth cone collapse, but fails to enhance dextran levels in the growth cone. Dextran also remains at background levels after a 5-min incubation with L1, a ligand which enhances neurite outgrowth. Bar, 20 μm.
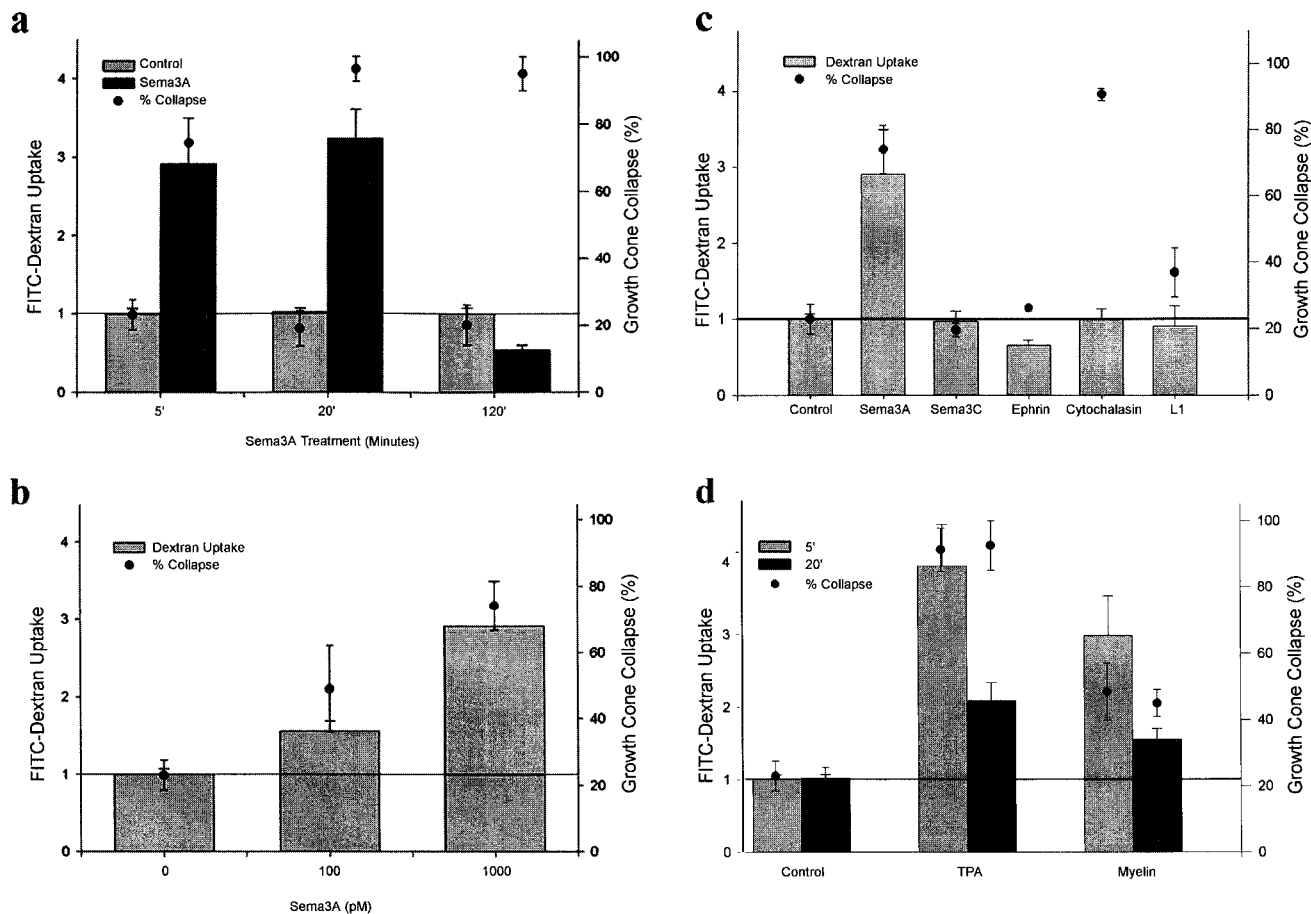
Figure 5. Ligand-stimulated endocytosis correlates with growth cone collapse. E7 chick DRG growth cones were exposed to test factors in the presence of FITC-dextran, washed, and rapidly fixed. Growth cones were counterstained with TRITC and quantified for total dextran levels as a proportion of the total protein level. (a) Time course of dextran accumulation in response to 1 nM Sema3A. (b) Dose curve of dextran accumulation 5 min after Sema3A application. (c) Dextran accumulation 5 min after the application of test ligands. (Sema3A and Sema3C, 1 nM; ephrin A5, 30 μg total membrane protein/ml; cytochalasin B, 2 μM; and L1Fc, 5 μg/ml.) (d) Dextran accumulation after TPA and myelin treatment. Note that TPA and CNS myelin stimulate FITC-dextran accumulation in the growth cone. (TPA, 1 μM; and myelin, 50 μg protein/ml).

Endocytosis Is Enhanced in Multiple Neuronal Cell Types by Growth Cone Collapsing Agents

We also tested the effect of repulsive ligands on dextran accumulation in RGC growth cones to determine if enhanced endocytosis in response to repulsive ligands may occur in multiple cell types. In addition to myelin and TPA, ephrin A5 effectively collapses RGC growth cones (Drescher et al., 1995). Conversely, RGCs lack the appropriate receptor to respond to Sema3A (Takahashi et al., 1998). We find that ephrin A5, TPA, and myelin all stimulate rapid RGC growth cone collapse and enhance dextran accumulation, whereas Sema3A fails to enhance RGC collapse or dextran accumulation (Fig. 6). These results demonstrate that active ligand-stimulated endocytosis may be a component of multiple physiologic axon repulsive pathways.

Dextran Is Localized to the Sites of Vacuoles and Ridges after Sema3A Treatment

To explore the relationship between dextran accumulation and Sema3A-induced linear and vacuolar structures, DRG growth cones were visualized by DIC microscopy after 5 min of FITC-dextran exposure in the presence of Sema3A (Fig. 7). The morphological correlates of dextran accumulations are similar to those of F-actin accumulations after Sema3A treatment (Fig. 1). Dextran accumulation is associated with several structures such as: punctate protrusions; membrane ridges; vacuoles with an indented reverse shadowcast appearance; and vacuoles with elevated, protrusive edges. After 5 min of Sema3A treatment, dextran is associated equally with punctate protrusions, and with elevated vacuoles. At later stages of collapse, dextran is found predominantly in elevated vacuoles (Fig. 7 m). At early and late time points, a minority of Sema3A is localized to membrane ridges and reverse shadowcast vacuoles.

Discussion

Fluid Phase Endocytosis Is Stimulated by Sema3A

We demonstrate for the first time that endocytosis is enhanced in the growth cone during ligand-induced collapse.
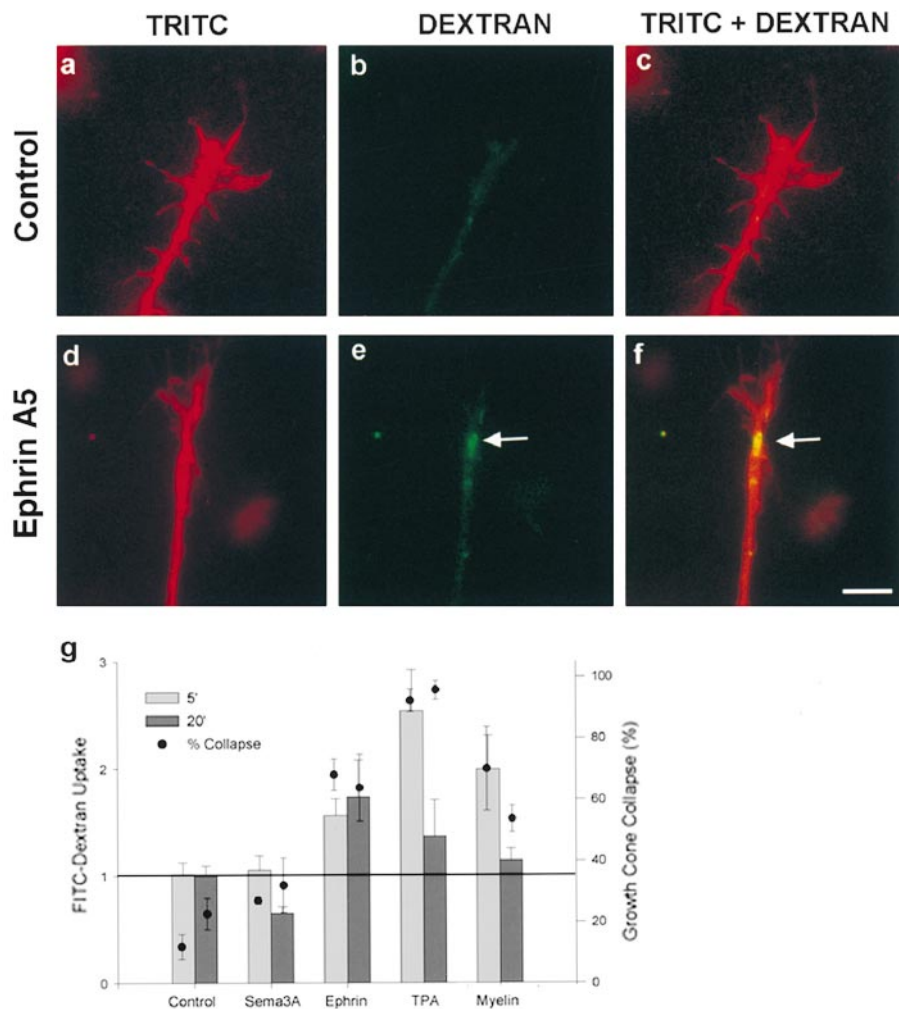
Figure 6. Ephrin A5 enhances endocytosis in RGCs. E7 chick RGC growth cones were exposed to medium (control) or ephrin A5 for 20 min in the presence of FITC-dextran, washed, and rapidly fixed. Medium (a–c) and ephrin A5 (d–f)–treated growth cones were stained with TRITC and examined for the total protein (a and d) or for FITC-dextran (b and e). Merged images (c and f) show the location of FITC-dextran uptake in the growth cone relative to total protein staining. Ephrin A5 enhances dextran accumulation in RGC growth cones (e). (g) Dextran levels as a proportion of total protein levels in the growth cone were quantified. Ephrin A5, TPA, and myelin cause RGC collapse and stimulate FITC-dextran accumulation in RGCs. Sema3A does not stimulate collapse or FITC-dextran accumulation in RGCs (Sema3A, 1 nM; ephrin A5 30 μg/ml; TPA, 1 μM; and myelin, 50 μg/ml). Bar, 20 μm.

The majority of dextran accumulates in punctate protrusions and larger elevated vacuolar structures within the growth cone lamelipodium. Elevated vacuoles represent unique sites of endocytosis that differ from the indented vacuolar structures, which mediate endocytic uptake in control growth cones. It is unclear if existing indented vacuolar structures and ruffles are transformed into elevated vacuoles in response to Sema3A, or if elevated vacuoles represent a new morphological structure stimulated by Sema3A. Such a determination will require live imaging and morphological analysis of the Sema3A-treated growth cones.

While the mechanism of endocytosis in Sema3A-treated growth cones is unclear, one possibility is that guidance cues are stimulating a specialized type of endocytosis, termed macropinocytosis. Macropinocytosis occurs when membrane ruffles fold back and fuse with the plasma membrane (Swanson and Watts, 1995). The highly motile character of newly formed membrane ridges suggests that they could be newly formed ruffles in the growth cone lamellipodium. Rac1 localization to Sema3A-induced membrane ridges provides a potential mechanism for their formation. Microinjection of activated rac1 into Swiss 3T3 fibroblasts stimulates membrane ruffling and macropinocytosis (Ridley et al., 1992), and the addition of serum or purified growth factors such as EGF or PDGF to nonneuronal cells stimulates cell-surface ruffling and fluid phase pinocytosis (Haigler et al., 1979). Morphologically, vacuoles formed during macropinocytosis can be quite large, from 1 to 5 μm in diameter, and this is consistent with the size of many of the DIC identifiable vacuoles after Sema3A treatment. These observations suggest a model whereby Sema3A acts through NP-1/plexin to stimulate the formation of rac1-positive ruffles, which mediate macropinocytosis in the growth cone.

It is also possible that other forms of adapter-mediated endocytosis contribute to dextran uptake. Receptor clustering and F-actin recruitment to phagocytic cups are characteristics of phagocytosis (Sheterline et al., 1984; Greenberg et al., 1991), and phagocytosis is inhibited by cytochalasin B (Zigmond and Hirsch, 1972). A role for rac1 also has been demonstrated in Fc gamma receptor–mediated phagocytosis. Fc gamma receptor–mediated phagocytosis is prevented by dominant negative rac1 in both 3T3 fibroblasts (Caron and Hall, 1998) and macrophages (Cox et al., 1997).

We also observe that TPA, myelin, and ephrin A5 stimulate dextran accumulation in collapsing growth cones, and this suggests that endocytosis is a common mechanism for physiologic growth cone collapse. The inability of cy-
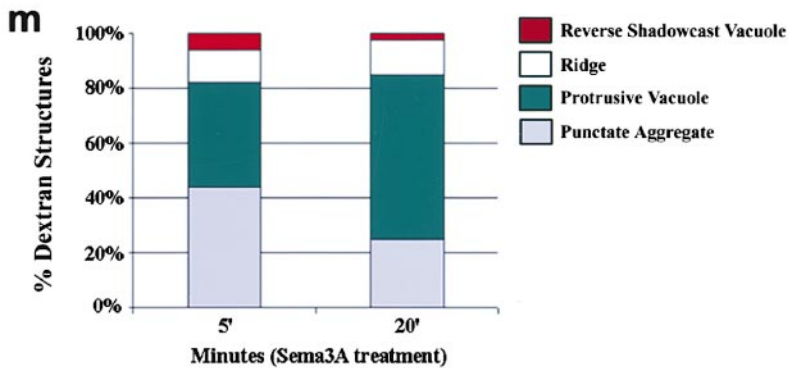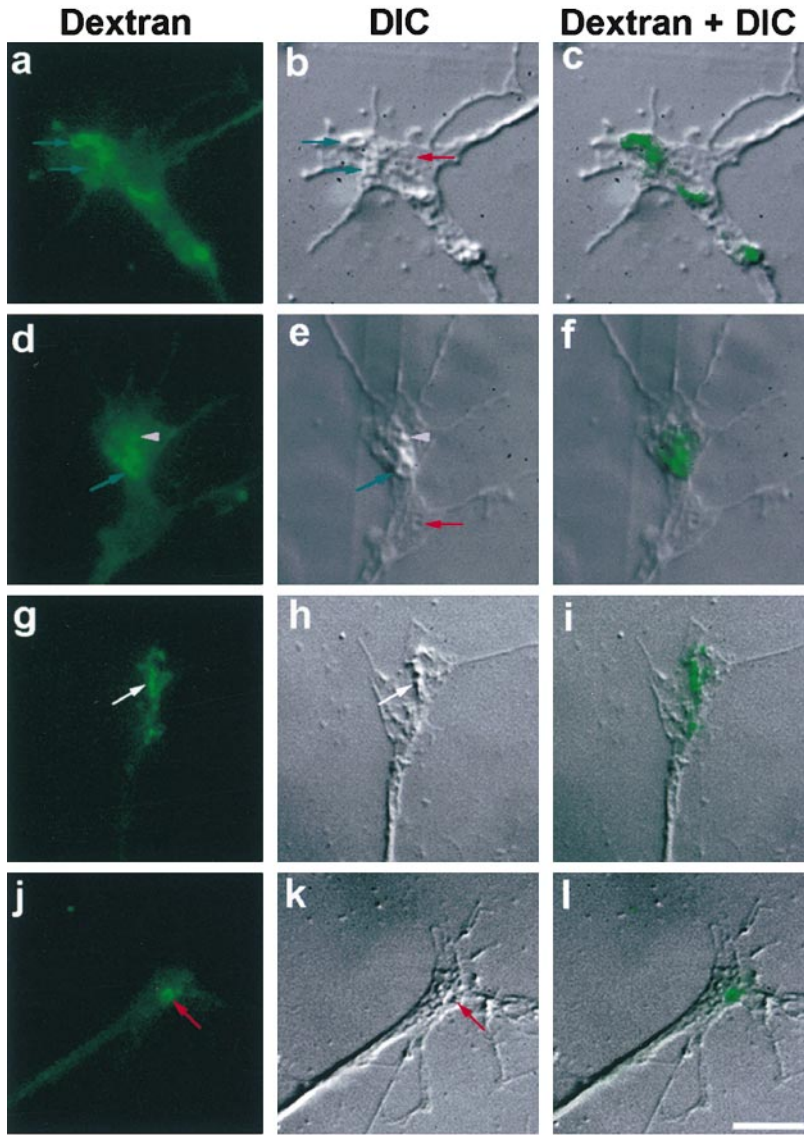
Dextran | DIC | Dextran + DIC

Figure 7. FITC-dextran is internalized at DIC identifiable ridges and vacuoles. Chick E7 DRG growth cones were treated with 1 nM Sema3A for 5 min in the presence of FITC-dextran. Four examples of FITC-dextran labeling (a, d, g, and j), and the paired DIC image (b, e, h, and k), show the localization of dextran within the growth cone. An FITC-dextran overlay on the DIC image (c, f, i, and l) shows the dextran localization relative to the DIC-identifiable structures. Dextran is found at sites of punctate aggregates (violet arrowheads), ridges (white arrows), reverse shadowcast vacuoles (red arrows), and protrusive vacuoles (green arrows). Two examples of reverse shadowcast vacuoles without dextran uptake are also labeled (b and e). (m) Analysis of dextran localization demonstrates that dextran can be found in all four types of structures at both 5 and 20 min. At later stages of collapse, dextran is predominantly associated with protrusive vacuoles. Bar, 20 μm.

tochalasin B to mimic the endocytic effects of ligands that cause growth cone collapse, has two implications. First, endocytosis is being stimulated by specific intracellular signaling events, and not just as a secondary consequence of changing growth cone morphology or actin disorganization. Second, endocytosis is not absolutely essential for collapse, rather it may be synergistic with actin rearrangements.

Endocytosis and Growth Cone Collapse

The growth cone is known to be a site of significant exocytosis and endocytosis in the basal state (Lockerbie et al., 1991; Diefenbach et al., 1999). During axonal growth, there is a dramatic increase in the total cell surface of the neuron, and the primary site of new membrane addition is the distal tip of the growth cone. The growth cone contains

stacks of intraneuronal membranes and large vacuolar structures that participate in endocytosis (Cheng and Reese, 1987). A role for endocytosis in growth cone function is also supported by studies on dynamin and amphiphysin (Mundigl et al., 1998).

The balance of exocytosis and endocytosis at the growth cone is likely to play a critical role in growth cone morphology, axonal extension, and navigational decisions. However, the regulation of growth cone membrane traffic by axon guidance cues has not previously been studied to any extent. Sema3A stimulation may tip a dynamic balance in favor of endocytosis at the growth cone plasma membrane. It has been demonstrated that the internalization of huge areas of plasma membrane accompany phagocytosis by nonneuronal cells. Classic experiments demonstrated that more than half of a macrophage's surface area can be internalized during the uptake of a phagocytic load (Werb and Cohn, 1972). The present data suggest that enhanced endocytosis contributes to growth cone collapse by internalization of the growth cone membrane. We have measured dextran accumulation during brief incubation periods, but we have not separately determined secretion and uptake rates. Therefore, decreased secretion rates might act synergistically with increased uptake rates to yield dextran accumulation and growth cone collapse.

Actin Filaments and Endocytosis

We demonstrate that F-actin is recruited to membrane ridges and vacuoles after Sema3A treatment. The formation of F-actin–rich structures strongly correlates with endocytic activity in a number of cell systems. F-actin–rich ruffles are stimulated by rac1 during pinocytosis in 3T3 fibroblasts (Ridley et al., 1992), and F-actin–rich ruffles and phagocytic cups form during phagocytosis in leukocytes (Cox et al., 1997). We show that the formation of actin-rich ruffles and vacuoles correlates with enhanced dextran accumulation in response to Sema3A, TPA, and myelin. Furthermore, dextran does not accumulate in response to cytochalasin B, which is a compound that fails to redistribute F-actin in an organized fashion. F-actin's translocation to specialized structures in the growth cone appears to play a critical role in the enhanced endocytosis.

Fan et al. (1993), observed a 50% reduction in the total F-actin in the growth cone. We also observe a decrease in filopodial F-actin. The decrease in filopodial F-actin induced by Sema3A is similar to that initiated by cytochalasin B. However, cytochalasin B causes a general disorganization of F-actin, whereas Sema3A causes its organized translocation to discrete structures. The inability of cytochalasin B to stimulate actin-rich lamellipodial structures and endocytosis may explain why growth cones continue to slowly advance in the presence of cytochalasin B (Letourneau et al., 1987) rather than halting as with Sema3A (Luo et al., 1993). We conclude that Sema3A induces coordinated cytoskeletal rearrangements that drive the formation of endocytic structures. The correlation between dextran accumulation at these endocytic structures and growth cone collapse suggests that enhanced endocytosis may contribute to the mechanism of growth cone collapse by Sema3A and other physiologic growth cone regulators.

References

Archer, F.R., P. Doherty, D. Collins, and S.R. Bolsover. 1999. CAMs and FGF cause a local submembrane calcium signal promoting axon outgrowth without a rise in bulk calcium concentration. *Eur. J. Neurosci.* 11:3565–3573.

Bandtlow, C.E., M.F. Schmidt, T.D. Hassinger, M.E. Schwab, and S.B. Kater. 1993. Role of intracellular calcium in NI-35-evoked collapse of neuronal growth cones. *Science.* 259:80–83.

Bar-sagi, D., and J.R. Feramisco. 1986. Induction of membrane ruffling and fluid phase pinocytosis in quiescent fibroblasts by ras proteins. *Science.* 233:1061–1068.

Bentley, D., and T.P. O'Connor. 1994. Cytoskeletal events in growth cone steering. *Curr. Opin. Neurobiol.* 4:43–48.

Caron, E., and A. Hall. 1998. Identification of two distinct mechanisms of phagocytosis controlled by different Rho GTPases. *Science.* 282:1717–1721.

Caroni, P., and M.E. Schwab. 1988. Two membrane protein fractions from rat central myelin with inhibitory properties for neurite growth and fibroblast spreading. *J. Cell Biol.* 106:1281–1288.

Chen, M.S., A.B. Huber, M.E. van der Haar, M. Frank, L. Schnell, A.A. Spillmann, F. Christ, and M.E. Schwab. 2000. Nogo-A is a myelin-associated neurite outgrowth inhibitor and an antigen for monoclonal antibody IN-1. *Nature.* 403:434–439.

Cheng, T.P.O., and T.S. Reese. 1987. Recycling of plasmalemma in chick tectal growth cones. *J. Neurosci.* 7:1752–1759.

Cox, D., P. Chang, Q. Zhang, P.G. Reddy, G.M. Bokoch, and S. Greenberg. 1997. Requirements for both Rac1 and Cdc42 in membrane ruffling and phagocytosis in leukocytes. *J. Exp. Med.* 186:1487–1494.

Dailey, M.E., and P.C. Bridgman. 1993. Vacuole dynamics in growth cones: correlated EM and video observations. *J. Neurosci.* 13:3375–3393.

Diefenbach, T.J., P.B. Guthrie, H. Stier, B. Billups, and S.B. Kater. 1999. Membrane recycling in the neuronal growth cone revealed by FM1-43 labeling. *J. Neurosci.* 19:9436–9444.

Doherty, P., E. Williams, and F. Walsh. 1995. A soluble chimeric form of the L1 glycoprotein stimulates neurite outgrowth. *Neuron.* 14:57–66.

Drescher, U.C., C. Kremoser, C. Handwerker, J. Loschinger, M. Noda, and F. Bonhoeffer. 1995. In vitro guidance of retinal ganglion cell axons by RAGS, a 25 kDa tectal protein related to ligands for Eph receptor tyrosine kinases. *Cell.* 82:359–370.

Fan, J., and J.A. Raper. 1995. Localized collapsing cues can steer growth cones without inducing their full collapse. *Neuron.* 14:263–274.

Fan, J., S.G. Mansfield, T. Redmond, P.R. Gordon-Weeks, and J.A. Raper. 1993. The organization of F-actin and microtubules in growth cones exposed to a brain-derived collapsing factor. *J. Cell Biol.* 121:867–878.

Goodman, C.S. 1996. Mechanisms and molecules that control growth cone guidance. *Annu. Rev. Neurosci.* 19:341–377.

Goshima, Y., F. Nakamura, P. Strittmatter, and S.M. Strittmatter. 1995. Collapsin-induced growth cone collapse mediated by an intracellular protein related to UNC-33. *Nature.* 376:509–514.

Goshima, Y., T. Kawakami, H. Hori, Y. Sugiyama, S.S. Takasawa, Y. Hashimoto, M. Kagoshima-Maezono, T. Takenaka, Y. Misu, and S.M. Strittmatter. 1997. A novel action of collapsin: collapsin-1 increases antero- and retrograde axoplasmic transport independently of growth cone collapse. *J. Neurobiol.* 33:316–328.

Grandpre, T., F. Nakamura, T. Vartanian, and S.M. Strittmatter. 2000. Identification of the Nogo inhibitor of axon regeneration as a reticulon protein. *Nature.* 403:439–444.

Greenberg, S., J. El Khoury, F. Di Virgilio, E.M. Kaplan, and S.C. Silverstein. 1991. Ca^{2+}-independent F-actin assembly and disassembly during Fc receptor-mediated phagocytosis in mouse macrophages. *J. Cell Biol.* 113:757–767.

Haigler, H.T., J.A. McKanna, and S. Cohen. 1979. Rapid stimulation of pinocytosis in human carcinoma cells A-431 by epidermal growth factor. *J. Cell Biol.* 83:82–90.

He, Z., and M. Tessier-Lavigne. 1997. Neuropilin is a receptor for the axonal chemorepellent semaphorin III. *Cell.* 90:739–751.

Igarashi, M., S.M. Strittmatter, T. Vartanian, and M.C. Fishman. 1993. G protein mediation of signals that cause growth cone collapse. *Science.* 259:77–79.

Jin, Z., and S.M. Strittmatter. 1997. Rac1 mediates collapsin-1-induced growth cone collapse. *J. Neurosci.* 17:6256–6263.

Kolodkin, A.L., D.V. Levengood, E.G. Rowe, Y.T. Tai, R.J. Giger, and D.D. Ginty. 1997. Neuropilin is a semaphorin III receptor. *Cell.* 90:753–762.

Kuhn, T.B., M.D. Brown, C.L. Wilcox, J.A. Raper, and J.R. Bamburg. 1999. Myelin and collapsin-1 induce motor neuron growth cone collapse through different pathways: inhibition of collapse by opposing mutants of Rac1. *J. Neurosci.* 19:1965–1975.

Letourneau, P.C., T.A. Shattuck, and A.H. Ressler. 1987. "Pull" and "push" in neurite elongation: observations on the effects of different concentrations of cytochalasin B and taxol. *Cell Motil. Cytoskel.* 8:193–209.

Li, M., A. Shibata, C. Li, P.E. Braun, L. McKerracher, J. Roder, S.B. Kater, and S. David. 1996. Myelin-associated glycoprotein inhibits neurite/axon growth and causes growth cone collapse. *J. Neurosci. Res.* 46:404–414.

Lin, C.H., C.A. Thompson, and P. Forscher. 1994. Cytoskeletal reorganization underlying growth cone motility. *Curr. Opin. Neurobiol.* 4:640–647.

Liu, Y., D.A. Fisher, and D.R. Storm. 1993. Analysis of the palmitoylation and membrane targeting domain of neuromodulin (GAP-43) by site-specific mutagenesis. *Biochemistry.* 32:10714–10719.

Lockerbie, R.O., V.E. Miller, and K.H. Pfenninger. 1991. Regulated plasma-lemmal expansion in nerve growth cones. *J. Cell Biol.* 112:1215–1227.

Luo, Y., D. Raible, and J.A. Raper. 1993. Collapsin: a protein in brain that induces the collapse and paralysis of neuronal growth cones. *Cell.* 75:217–227.

McKerracher, L., S. David, J.L. Jackson, V. Kottis, R. Dunn, and P.E. Braun. 1994. Identification of myelin-associated glycoprotein as a major myelin-derived inhibitor of neurite outgrowth. *Neuron.* 13:805–811.

Mundigl, O., G.C. Ochoa, C. David, V.I. Stepnev, A. Kabanov, and P. DeCamilli. 1998. Amphiphysin I antisense oligonucleotides inhibit neurite outgrowth in cultured hippocampal neurons. *J. Neurosci.* 18:93–103.

Prinjha, R., S.E. Moore, M. Vinson, S. Blake, R. Morrow, D. Michalovich, D.L. Simmons, and F.S. Walsh. 2000. Inhibitor of neurite outgrowth in humans. *Nature.* 403:383–384.

Puschel, A.W. 1996. The semaphorins: a family of axonal guidance molecules? *Eur. J. Neurosci.* 8:1317–1321.

Ridley, A.J., H.F. Peterson, C.L. Johnston, D. Kiekmann, and A. Hall. 1992. The small GTP-binding protein rac regulates growth factor induced membrane ruffling. *Cell.* 70:401–410.

Seilheimer, B., and M. Schachner. 1988. Studies of adhesion molecules mediating interactions between cells of peripheral nervous system indicate a major role for L1 in mediating sensory neuron growth on Schwann cells in culture. *J. Cell Biol.* 107:341–351.

Sheterline, P., J.E. Rickard, and R.C. Richards. 1984. Fc receptor-mediated phagocytic stimuli induce transient actin assembly at the early stage of phagocytosis in neutrophil leukocytes. *Eur. J. Cell Biol.* 34:80–87.

Song, H., G. Ming, Z. He, M. Lehmann, L. McKerracher, M. Tessier-Lavigne, and M. Poo. 1998. Conversion of neuronal growth cone responses from repulsion to attraction by cyclic nucleotides. *Science.* 281:1515–1518.

Swanson, J.A., and C. Watts. 1995. Macropinocytosis. *Trends Cell Biol.* 5:424–428.

Takahashi, T., F. Nakamura, Z. Jin, R.G. Kalb, and S.M. Strittmatter. 1998. Semaphorins A and E act as antagonists of neuropilin-1 and agonists of neuropilin-2 receptors. *Nat. Neurosci.* 1:487–493.

Takahashi, T., A.E. Fournier, F. Nakamura, L.-H. Wang, Y. Murakami, R.G. Kalb, H. Fujisawa, and S.M. Strittmatter. 1999. Plexin-neuropilin-1 complexes form functional semaphorin-3A receptors. *Cell.* 99:59–69.

Tamagnone, L., S. Artigiani, H. Chen, H. Zhigang, G.-L. Ming, H.-J. Song, A. Chedotal, M.L. Winberg, C.S. Goodman, M. Poo, M. Tessier-Lavigne, and P.M. Comoglio. 1999. Plexins are a large family of receptors for transmembrane, secreted, and GPI-anchored semaphorins in vertebrates. *Cell.* 99:71–80.

Walter, J., B.K. Kern-Veits, J. Huf, B. Stolze, and F. Bonhoeffer. 1987. Recognition of position-specific properties of tectal cell membranes by retinal axons in vitro. *Development.* 101:685–696.

Werb, Z., and Z.A. Cohn. 1972. Plasma membrane synthesis in the macrophage following phagocytosis of polystyrene latex particles. *J. Biol. Chem.* 247:2439–2446.

Zigmond, S.H., and J.G. Hirsch. 1972. Effects of cytochalasin B on polymorphonuclear leukocyte locomotion, phagocytosis and glycolysis. *Exp. Cell Res.* 73:383–393.